CMNE/CILAMCE 2007
Porto, 13-15 Junho, 2007

OPTIMIZATION OF IMPACT DAMPING FOR A NON-IDEAL STRUCTURAL SYSTEM

Marcelo A Silva*[1], Reyolando M L R F Brasil[2]

1 Department of Structural and Geotechnical Engineering - Polytechnic School – The University of Sao Paulo (PEF/EPUSP/USP), Caixa Postal 61548, CEP 05.424-970
Sao Paulo-SP., Brazil, E-mail: m_araujo_silva@uol.com.br

2 Department of Structural and Geotechnical Engineering - Polytechnic School - The University of Sao Paulo (PEF/EPUSP/USP), Caixa Postal 61548, CEP 05.424-970
Sao Paulo-SP., Brazil, E-mail: rmlrdfbr@usp.br

Key words: Optimization, impact dampers, non-linear dynamics, Sommerfeld effect, non-ideal systems.

Summary. *We intend, in this work, to present some research results on the optimization of the efficiency of an impact damper for a non-ideal structural system. In the model, the impact vibration absorber is, basically, a small free mass inside a box carved in the structure that undergoes undamped linear motions colliding against the walls of the box. Whenever the mass shocks against the walls of the box, an exchange of kinetic energy between the mass and the structure may be used to control the amplitude of the dynamic response of the structure. In this work, the structure is considered to be excited by a non-ideal power source, a DC electric motor installed on it, which suffers the Sommerfeld effect. A non-ideal power source is one that suffers interaction with the motion of the structure as opposed to an ideal source whose amplitude and frequency are fixed, independent of the displacements of the structure. Here, we compute the dynamic response of the system using step-by-step numerical integration of the equations of motion, obtained through a Lagrangian formulation. The optimization problem is defined considering as the objective function the maximum amplitude of the structure displacement, while the design variables are the weight of the free mass and the width of the carved box. Using the augmented Lagrangian method, we formulate several optimization problems and, solving them, we get the best design to maximize the efficiency of the impact damper.*

1. INTRODUCTION

Vibro-impact systems have oscillating parts colliding against other vibrating components or rigid walls. An impact damper is a vibro-impact system of practical importance. In this case, the vibration of the primary system is controlled by the momentum transferred through collisions with the secondary system, a free mass that displaces back and forth shocking against the walls of a carved box [1][2]. An example of a structural system with an impact damper is the motor foundation structure shown in Fig. 1. In this figure we can see that the primary system is composed by two columns, a rigid beam and a motor installed on it. The columns present stiffness k and height h, the rigid beam has mass m_1. Generalized coordinate q_1 is related to the horizontal displacement of the mass fixed to the top of the columns. The motor has a rotating mass m_2 with eccentricity e and polar moment of inertia J_2. The angular displacement of m_2 is given by generalized coordinate q_2. The secondary system is given by the free mass m_3, which displaces back and worth inside the carved box shocking against its walls. The carved box has length d and the position of this mass is given by generalized coordinate q_3. If the free mass exchanges kinetic energy with the primary system, it can reduce drastically the displacements of the motor foundation structure, working as an impact damper.

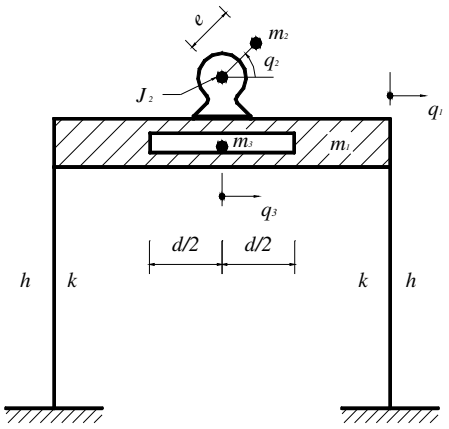

Fig.1. Model of a motor foundation structure

A simple ideal model supposes a periodic forcing function due to an external source, which is not perturbed by the motion of the structure. However, in practical situations, the dynamics of the forcing system cannot be considered as given a priori, and it must be taken as also a consequence of the dynamics of the whole system [3][4]. If the forcing system has a limited energy source, as that provided by an electric motor, for example, its own dynamics is influenced by that of the oscillating system which is being forced. This increases the number of degrees of freedom, and is called a non-ideal problem. The system shown in Fig. 1 is a non-ideal system, since the degree of freedom of motor (q_2) is influenced by the structure displacement (q_1).

The first type of non-ideal problem presented in the literature is the well-known

Sommerfeld Effect, homage to the first researcher to observe it in 1902. This phenomenon was largely studied by Kononenko [5] in a work basically dedicated to non-ideal power sources. In that work, a cantilever beam, clamped in one extremity, with a motor installed on its free extremity, was analyzed experimentally with the objective of detecting the interaction between the motor and the beam. The system presented unstable motions near resonance and the experiment could not reproduce the resonance curve. Starting from those results, researchers that considered non-ideal sources of energy in their models, for certain parameters, could not reproduce the resonance curves without discontinuities, like that observed for ideal models. It was not possible to find stable solutions in the resonance region, leading to jumps of motor frequencies and the structure displacements.

Analyzing the region before the resonance by a graph of motor frequency versus structure displacement (Fig. 2), one can note that when the power given by the source to the motor is increased, the motor frequency is also increased. It is important to clarify here that each point is Fig. 2 is related to a fixed given power level. However, as the motor frequency approachs the resonance region, the power source must supply more energy to increase the motor rotation, as part of this energy is being consumed by the motion of the structure. A large change of power supplied to the motor results in just small changes in its frequency, and a large increase of the structure displacements.

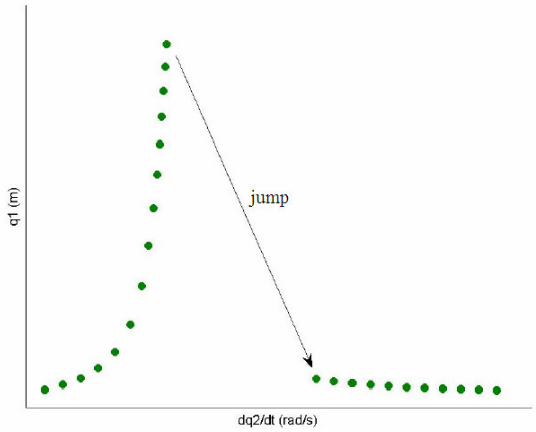

Fig.2. Displacement of the structure as function of the frequency of the motor, as the motor energy is increased

So, near to the resonance region, one can note that the additional power given to the motor only increases the structure displacement having little effect on the motor frequency. Right after the resonance, the structure displacement decreases drastically, as well as the motor frequency increases drastically. There is a “jump” in the resonance curve. The increase of power required and the “jump” near the resonance region is called Sommerfeld effect. Fig. 3 shows what happens with the structure energy as the motor energy is increased in a non-ideal system.

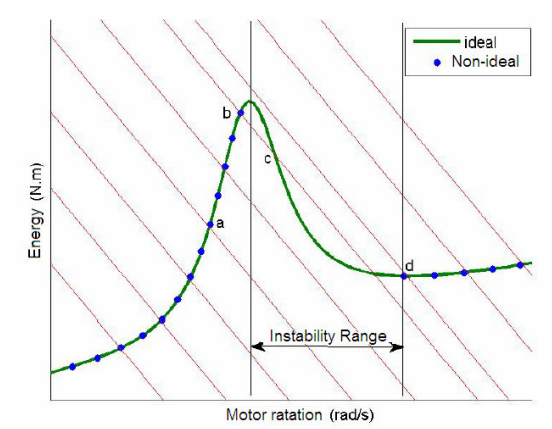

Fig.3. Energy of the structure as function of the frequency of the motor, as the motor energy is increased

As we stated before, an unbalanced non-ideal DC motor foundation structure that suffers the Sommerfeld effect uses the energy supplied to the motor, before the resonance region, to increase the motions of the supporting structure. An efficient impact damping may tone down or even suppress that undesired phenomena without dissipation of energy.

The main goal of this paper is to formulate and solve optimization problems where the objective is to minimize the structure displacements in the stationary regime, properly designing the carved gap and the free mass.

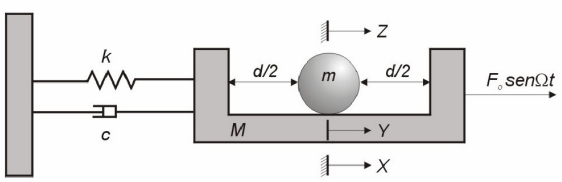

Fig.4. Model of SPID proposed by Popplewell et al [6]

2. IMPACT DAMPERS

There are various types of impact dampers (ID), starting with a single degreeof freedom one. The simplest ID is called Single Particle Impact Damper (SPID) or Single Unit Impact Damper. In this ID there is only one free mass that shock against the walls of a box. Popplewell et al [6] and Bapat et al [7] studied theoretically and experimentally the stable periodic vibrations of a SPID excited by a sinusoidal load, finding a reasonable correlation between the theory and practice. A reproduction of the model proposed by those authors is shown in Fig. 4.

More recently Duncan et al [8] accomplished a numerical investigation of the performance of the damping of one SPID of vertical vibrations (Fig 5) for a vast interval of frequencies, amplitudes of vibrations, damping rates and other parameter.

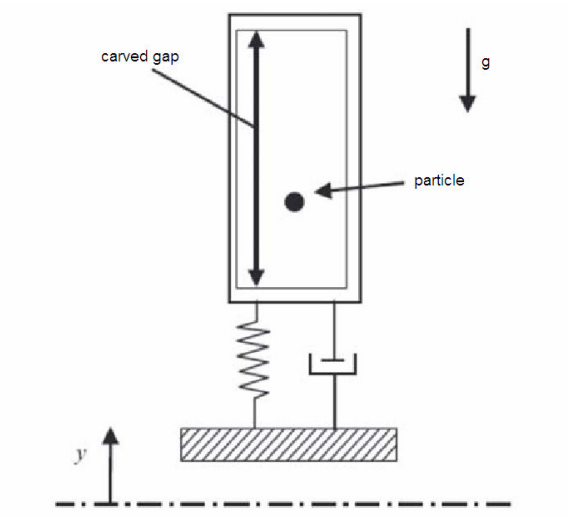

Fig.5. Model of SPID studied by Duncan et al [8]

According to Bapat and Sankar [9], and latter confirmed by Popplewell and Liao [10], the efficiency of an ID decreases with the increase of the damping rate of a given structure, and it reaches the maximum when the rate between the frequency of loading and the natural frequency of vibration of the structure approaches one, that is, in resonance. Popplewell and Liao [10] gave some expressions to compute the optimum gap (d) for a SPID design. There are several definitions of how to compute the efficiency of an ID, such as the rate between the maximum displacement with and without the ID, the rate between the maximum dynamic displacement and the static displacement, etc. In the present work, the authors consider the first definition given above to analyze if the ID is efficient or not.

Starting from the basic idea of the SPID, researchers developed others variation of ID, such as the Multi-Particle Impact Damper (MPID), shown in Fig. 6. This ID contains a big quantity of particles, producing dissipation of energy also through the friction between the particles. Several authors have studied the behavior of the MPID, among them we can mention Saeki [11] and Marhadi and Kinra [12]. The studies conducted by these authors analyzed the influence of the size of the box, the kind of granular material of particles and the specific mass in the performance of the ID.

We should also describe the Bean Bag Impact Damper (BBID), name given because of the similarity with a bean bag, which consists of several particles confined in side a plastic bag. According to Popplewell and Semercigil [13], which investigated the performance of the BBID shown in Fig. 7, it has the advantage of minimize the noise by the fact of the bag has a

certain flexibility of shape and increase the damping due to the interaction between the particles.

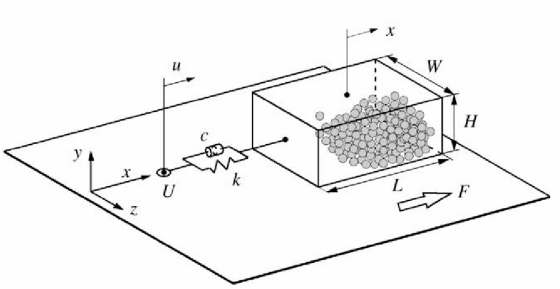

Fig.6. Model of MPID proposed by Saeky [11]

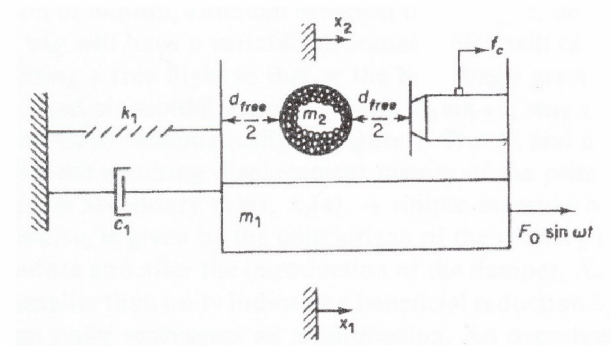

Fig.7. Model of Bean Bag Impact Damper

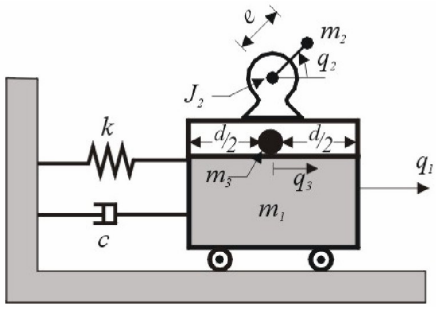

Fig. 8. Non-ideal model with impact damper [14]

Note that the entire IDs showed before present an external ideal load given by a sinusoidal function, which is not influenced by the structure displacement. However, in this work we are going to consider a non-ideal model, where the interaction between the loading and the vibrating system is taken in consideration. The non-ideal system is obtained replacing the sinusoidal external loading by a rotor attached to the structure and supplied by a motor. The

mathematical model of a non-ideal system with an impact damper, developed by Feitosa [14], is shown in Fig 8. This model is the one that will be studied and optimized in the present work.

3. THE EQUATIONS OF MOTION

In this section we are going to deduce the equations of motion for the system given by Figs. 1 and 8. We first derive the equations of motion for the non-controlled model that is made using the Lagrange's equations. We consider the Rayleigh's dissipation function to model the viscous structural damping, as well as to model the mechanisms of supplying and dissipating (internal friction) of energy in the motor, as:

$$\Im = \frac{1}{2}(c\dot{q}_1^2 + b\dot{q}_2^2) - a\dot{q}_2 \tag{1}$$

where c is the constant of the viscous structural damping, while a and b are motor constants given by the manufacturer.

Introducing the total potential energy, the kinetic energy and the dissipation function into the Lagrange's equations, we obtain the following pair of non-linear ordinary differential equations of motion for the non-controlled model:

$$M\ddot{q}_1 + c\dot{q}_1 + kq_1 = S(\ddot{q}_2 \sin q_2 + \dot{q}_2^2 \cos q_2) \tag{2}$$

$$J\ddot{q}_2 + b\dot{q}_2 - a = S(\ddot{q}_1 \sin q_2 - g \cos q_2) \tag{3}$$

where $M = m_1 + m_2$, $S = m_2 e$ and $J = J_2 + m_2 e^2$.

Next, we introduce the impact control by means of the third free mass m_3. This mass is free to displace back and forth inside the carved box, fixed to the structure. This leads to an additional degree of freedom. We denote q_3 the displacement of this point mass, which is bounded by the moving walls of the carved gap. The additional equation of motion for this coordinate, assuming that there is no friction between the mass and the box surface, is the uncoupled second order homogeneous differential equation

$$\ddot{q}_3 = 0 \tag{4}$$

When we have

$$\left|q_3 - q_1\right| \geq d/2 \tag{5}$$

it means mathematically that the impact already happened. Thus we have to compute the velocities $\dot{q}_{1a}$ and $\dot{q}_{3a}$, at the time t_a, immediately *after* each impact between the mass m_3 and the main structure of mass m_1. To calculate $\dot{q}_{1a}$ and $\dot{q}_{3a}$ we consider inelastic collisions with restitution coefficient $0 < r < 1$. This quantity is defined as the ratio between the differences of velocities of the masses when they approach each other, just *before* the collision, and the same

difference when they separate one from other, just *after* the impact. So r is computed as:

$$r = -\frac{\dot{q}_{1a} - \dot{q}_{3a}}{\dot{q}_{1b} - \dot{q}_{3b}} = \frac{-(velocity\ of\ \ separation)}{(velocity\ of\ \ approach)} \tag{6}$$

As we have two unknown velocities after impact to determine, we need another equation besides Eq. (6). It is the statement of the conservation of the linear momentum:

$$m_1 \dot{q}_{1a} + m_3 \dot{q}_{3a} = m_1 \dot{q}_{1b} + m_3 \dot{q}_{3b} \tag{7}$$

Solving Eqs. (6) and (7), we obtain the initial velocities, just *after* the impact, to integrate the equations (2) to (4):

$$\dot{q}_{1a} = \frac{(m_1 - r m_3)\dot{q}_{1b} + m_3(1+r)\dot{q}_{3b}}{m_1 + m_3}, \qquad \dot{q}_{3a} = \frac{(m_3 - r m_1)\dot{q}_{3b} + m_1(1+r)\dot{q}_{1b}}{m_1 + m_3}. \tag{8}$$

For a given time t after a certain impact and before the following one, we determine velocities and displacements by simple integration of Eq. (4).

4. THE AUGMENTED LAGRANGIAN METHOD

To solve the structural optimization problems formulated in this paper is necessary the adoption of optimization algorithms that deal with static and dynamic constrains, as well as non-linear functions. A non-linear optimization problem with static and dynamic constrains is presented as follow: find the design variables $\boldsymbol{x} \in \boldsymbol{R}^n$ that minimize the non-linear objective function $f(\boldsymbol{x})$ subjected to the non-linear constrain functions:
Static

$$g_i(\boldsymbol{x}) = 0; \quad i = 1, l \tag{9}$$

$$g_i(\boldsymbol{x}) \le 0; \quad i = l+1, m \tag{10}$$

and dynamic, $\forall\ t \in [t_0, t_f]$,

$$g_i(\boldsymbol{x}, t) = g_i(\boldsymbol{x}, z(t), \dot{z}(t), \ddot{z}(t), t) = 0; \quad i = m+1, l' \tag{11}$$

$$g_i(\boldsymbol{x}, t) = g_i(\boldsymbol{x}, z(t), \dot{z}(t), \ddot{z}(t), t) \le 0; \quad i = l'+1, m' \tag{12}$$

In dynamics of structures, the displacement vector $z(t)$ must satisfy the equations of motion, a system of second-order ordinary differential equations:

$$\boldsymbol{M}(\boldsymbol{x}, \ddot{z}, \dot{z}, z, t)\ddot{z}(t) + \boldsymbol{C}(\boldsymbol{x}, \ddot{z}, \dot{z}, z, t)\dot{z}(t) + \boldsymbol{R}(\boldsymbol{x}, \ddot{z}, \dot{z}, z, t) = \boldsymbol{p}(\boldsymbol{x}, \ddot{z}, \dot{z}, z, t) \tag{13}$$

The initial conditions are $\dot{z}(t_0) = \dot{z}_0$ and $z(t_0) = z_0$, where $\boldsymbol{M}(\boldsymbol{x}, \ddot{z}, \dot{z}, z, t)$ and $\boldsymbol{C}(\boldsymbol{x}, \ddot{z}, \dot{z}, z, t)$ are, respectively, the mass and damping matrix, the vector $\boldsymbol{R}(\boldsymbol{x}, \ddot{z}, \dot{z}, z, t)$ is the generalized elastic force and $\boldsymbol{p}(\boldsymbol{x}, \ddot{z}, \dot{z}, z, t)$ is the generalized force vector. Equations (9) and (10) include,

for example, limits of the design variables. Equations (11) and (12) represent constraints with dynamic responses such as the maximum and minimum values of the displacements $z(t)$, dynamic strain and stress. The initial and final times are t_0 and t_f, respectively.

During the designing process, a set of parameters, denoted design variables $\boldsymbol{x}$, are selected to define the system that will be projected. Once specified the design variables, the vector $z(t)$ is determined by Eq. (13). The displacements are called state variables, as they determine the structure configuration for every $t \in [t_0,t_f]$, and Eq. (13) is the state equation. The constraints with dynamic responses are explicit functions of state variables and implicit functions of the design variables. Usually, in structural optimization problems with dynamic constraints, the state variables vector is denoted $z(t)$. As one can note, in this work we also use the notation $\boldsymbol{q}(t)$ for the displacement vector.

There are several methods to solve the problem defined by the equations (9) to (13). We treat this problem using the augmented Lagrangian method. The Lagrangian functional is created using the objective and the constraint functions, associated to the Lagrange multipliers and penalty parameters:

$$\Phi(\boldsymbol{x},\boldsymbol{u},\boldsymbol{r}) = f(\boldsymbol{x}) + P(\boldsymbol{g}(\boldsymbol{x}),\boldsymbol{u},\boldsymbol{r}) \tag{14}$$

$P(\boldsymbol{g}(\boldsymbol{x}),\boldsymbol{u},\boldsymbol{r})$ is a penalty functional, $\boldsymbol{u} \in \boldsymbol{R}^{m'}$ and $\boldsymbol{r} \in \boldsymbol{R}^{m'}$ are, respectively, the Lagrange multipliers and the penalty parameters. It is possible to determine $\boldsymbol{u}^*$ and $\boldsymbol{r}^*$ so that the minimum point $\boldsymbol{x}^*$ of the functional defined in (14) is the minimum point of the problem defined by Eqs. (9) to (13). As we use iterative methods to find $\boldsymbol{u}^*$ and $\boldsymbol{r}^*$ so it is necessary to use a stopping criterion.

The augmented Lagrangian method defines procedures for updating penalty parameters and Lagrange multipliers. This method can be simply described by the algorithm:

Step 1. set k=0, estimate vector $\boldsymbol{u}$ and $\boldsymbol{r}$;

Step 2. minimize $\Phi(\boldsymbol{x},\boldsymbol{u}^k,\boldsymbol{r}^k)$ with respect to $\boldsymbol{x}$. Let $\boldsymbol{x}^k$ be the best point obtained in this step;

Step 3. if the stopping criterion is satisfied, stop the iterative process;

Step 4. update $\boldsymbol{u}^k$, and $\boldsymbol{r}^k$, if it is necessary;

Step 5. set k=k+1 and go to step 2.

The multipliers method is really simple and its essence is contained in steps 2 and 4. The functional (14) can be defined in several ways.

In the present work, the Lagrangian functional adopted to solve the problem with dynamic response, defined by the Eqs. (9) to (13), is defined by:

$$\begin{aligned}\Phi(\boldsymbol{x},\boldsymbol{\theta},\boldsymbol{r}) = f(\boldsymbol{x}) + \frac{1}{2}\left\{\sum_{i=1}^{l} r_i\left(g_i(\boldsymbol{x})+\theta_i\right)^2 + \sum_{i=l+1}^{m} r_i\left(g_i(\boldsymbol{x})+\theta_i\right)_+^2\right\} + \\ \frac{1}{2}\int_{t_0}^{t_f}\left\{\sum_{i=m+1}^{l'} r_i\left(g_i(\boldsymbol{x},t)+\theta_i\right)^2 + \sum_{i=l'+1}^{m'} r_i\left(g_i(\boldsymbol{x},t)+\theta_i\right)_+^2\right\}dt\end{aligned} \tag{15}$$

In the Eq. (15) r_i are the penalty parameters and θ_i define the Lagrangian multipliers as $u_i = r_i\theta_i$, for i=1,...,m'. Note that, in (15), the dynamic constraint functions are integrated at the

time interval and combined with the objective function to obtain the Lagrangian functional. At the steps 2 and 3 it is necessary to adopt a stopping criterion. Here, we consider the following criterion:

$$k<p, \tag{16}$$

where p is maximum number of iterations, and

$$\left\|\nabla\Phi(\boldsymbol{x}^k,\boldsymbol{u}^k,\boldsymbol{r})\right\| \le \varepsilon \text{ and} \tag{17}$$

$$\begin{aligned} K_b = max\{ & \max_{1\le i\le l} | g_i(\boldsymbol{x}^{(k)}) |; \max_{l+1\le i\le m} | max(g_i(\boldsymbol{x}^{(k)}),-\theta_i) |; \\ & \max_{1\le i\le l'} (\max_{t_0\le t\le t_f} | g_i(\boldsymbol{x}^{(k)},t) |); \max_{l'+1\le i\le m'} (\max_{t_0\le t\le t_f} | max(g_i(\boldsymbol{x}^{(k)},t),-\theta_i(t)) |) \} \le \varepsilon \end{aligned} \tag{18}$$

In (18) K_b is the maximum constraint violation and in (17) and (18) ε is the tolerance. If the algorithm is not converging, the condition (16) states a finite number of iterations. Arora et al [15] noted in several examples analyzed that the best value for p is $2n$. The process of updating the Lagrange multipliers and penalty parameters and more details on the adopted algorithm can be found in Arora et al [15] and Chahande and Arora [16].

A computation program was developed by the authors, based on this augmented Lagrangian method. The following numerical methods were utilized to implement this method:

- to solve the equations of motion (12), we use the Newmark's method or 5th order Runge-Kutta's method;.
- related to unconstrained minimization (step 2), we use conjugated gradient method with Armijo line search is;
- to calculate the gradient vector, we use finite difference method;
- to integrate (14), we use the Simpson rule;
- to solve linear systems, we use Cholesky decomposition.

Originally the standard Newmark's method was developed for linear equations. However, in the present work, equations of motion are non-linear equations. So we developed a Newmark's method conjugated with the Newton-Raphson's method. Instead of obtaining a linear equation to be solved in each instant of time, as in classical Newmark's method, we get a non-linear equation, which is solved by the Newton-Raphson's method. In Section 6 we are going to discuss the performance of this Newmark's method compared with the performance of the 5th order Runge-Kutta's method.

5. THE OPTIMIZATION PROBLEMS

Consider the elevated machine foundation showed in Figure 1. The objective is to design a carved box and a free mass that minimize the maximum structure displacement in the steady state regime, in other words, minimize the maximum displacement of the degree of freedom q_1, properly varying the parameters d and m_3. Thus, the natural design variables of this

problem are the carved gap d, considered here as the design variable x_1, and the mass m_3, considered as design variable x_2. Since q_1 is a state variable, it can not be directly the objective function because the objective function is a function of the design variables. So, how to minimize q_1? To avoid this matter we create an artificial design variable x_3, which is the maximum value allowable to q_1 and also the objective function. The design variable vector is $\boldsymbol{x}^{\mathrm{T}} = \{x_1 \;\; x_2 \;\; x_3\} \equiv \{d \;\; m_3 \;\; \max(q_1)\}$.

The optimization problem is to determine $\boldsymbol{x} \in \Re^3$ that minimize the objective function

$$f(\boldsymbol{x}) = x_3 \tag{19}$$

subjected to the static constraints

$$\{\, d \geq 0 \,\} \equiv \{g_1(\boldsymbol{x}) = -\, x_1\}, \tag{20}$$

$$\{\, m_3 \geq 0 \,\} \equiv \{g_2(\boldsymbol{x}) = -\, x_2\}, \tag{21}$$

subjected to the dynamic constraint

$$\{q_1 \leq x_3\} \equiv \{g_3(\boldsymbol{x},t) = q_1 - x_3, \;\; \forall\, t \in [t_0,t_f]\}. \tag{22}$$

The state variables must satisfy the state equations, given by Eqs. (2) to (4) and (8). It is important to remember that the motor constant a assumes several values in a given interval $[a_0,a_f]$, according to the power supplied to the motor and the discretization adopted to the interval. For each value of a we have one solution for the equations of motion.

As we stated before, the objective is to minimize q_1 in the stationary regime. So when we minimize x_3 we are minimizing q_1 in both transient and stationary regime. Maybe, it could be better to give emphasis only in the steady state regime. So we define now q_{s1}, $\forall\, t \in [t_s,t_f]$, that is the displacement q_1 in the stationary regime and t_s is the time when the stationary regime starts. Searching the best formulation for the problem of minimizing the displacement q_{s1}, we define others objective functions, as follow:

$$f(\boldsymbol{x}) = \max_{a_0 \leq a \leq a_f} \; \max_{t \in [t_s,t_f]} \left| q_{s1} \right| \tag{23}$$

$$f(\boldsymbol{x}) = \sum_{a=a_0}^{a_f} \max_{t \in [t_s,t_f]} \left| q_{s1} \right| \tag{24}$$

$$f(\boldsymbol{x}) = \frac{1}{2} \sum_{a=a_0}^{a_f} \max_{t \in [t_s,t_f]} \left| q_{s1} \right|^2 \tag{25}$$

$$f(\boldsymbol{x}) = 2 \sum_{a=a_0}^{a_f} \max_{t \in [t_s,t_f]} \left| q_{s1} \right|^{0.5} \tag{26}$$

When we use Eq. (23) as the objective function, the constraint function, given by Eq. (22), must be computed $\forall\ t \in [t_s,t_f]$. In case of using one of the objective functions given by Eqs. (24) to (26), the constraint (22) is suppressed and the design variable vector becomes $\boldsymbol{x} \in \Re^2$, such as $\boldsymbol{x}^T = \{x_1\ \ x_2\} \equiv \{d\ \ m_3\}$.

There are several methods to solve the problems defined by equations (19) to (26), such as the Sequential Quadratic Program (SQP) and the Augmented Lagrangian Method. As we wrote before, in this work we use the Augmented Lagrangian Method as described in Section 4.

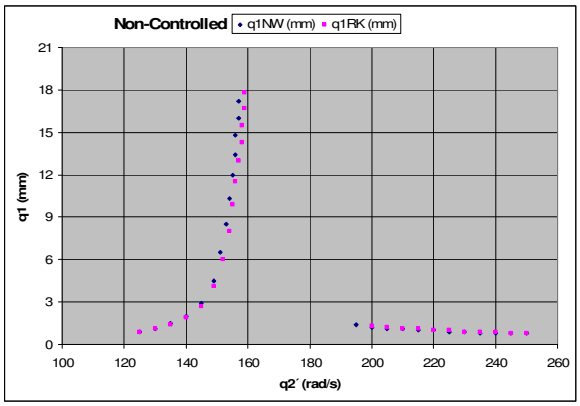

Fig. 9. Comparison between Newmark (NW) and 5th order Runge-Kutta's (RK) methods for non-controlled problem

6. NUMERICAL RESULTS AND COMMENTS

We adopted the following numerical values for the structural parameters: k = 49152 N/m and M = 2 kg, leading to natural frequency ω = 156.767 rad/s; S = 0.001 kg.m; $J = 1.776\text{x}10^{-4}$ kg.m^2; c = 3.1353 N.s/m, equivalent to 0.5% of the critical damping. In Eqs. (8) we consider $m_1 = M$. The motor parameters are a rising from a_0 = 0.25 up to a_f = 0.50, with step of 0.01, and b = 0.002 N.m.s. For the dynamic analysis, the initial values for the state variables are:

$$\boldsymbol{q}^T(0) = \{0 \quad 0 \quad d/2\} \ \text{ and } \ \dot{\boldsymbol{q}}^T(0) = \{0 \quad 0 \quad 0\} \tag{27}$$

and the time interval is $t \in [0,10]$ s, discretized into 4801 grid points, equally spaced. As we stated before, the values of d and m_3 will be computed by solving the optimizations problems already defined.

The first analysis we addressed was to verify what method, Newmark or 5th order Runge-Kutta, is more precise and stable for the proposed problems. So we solve the non-controlled problem, considering only the degrees of freedom q_1 and q_2, and plotted the results in a graph as shown in Fig. 9. We can see in this figure that the precision of both methods is basically the same, but we noted, based on others results, that Newmark is more stable, specifically near to

the resonance region. It is important to clarify here that each point in that graph is related to a given value of a, and it means a certain value of power supplied to the motor. One can note that we have 26 grid points in that graph, which is the discretization presented above for the values of a. As we increase the value of a we generate points from left to right in that figure. So, left points are related to lower level of power. Based on the results of Fig. 9 and the considerations presented above, we chose the Newmark's method to solve the equations of motion in the next results shown in this work. The curves shown in Fig. 9 are also denoted as the resonance curve.

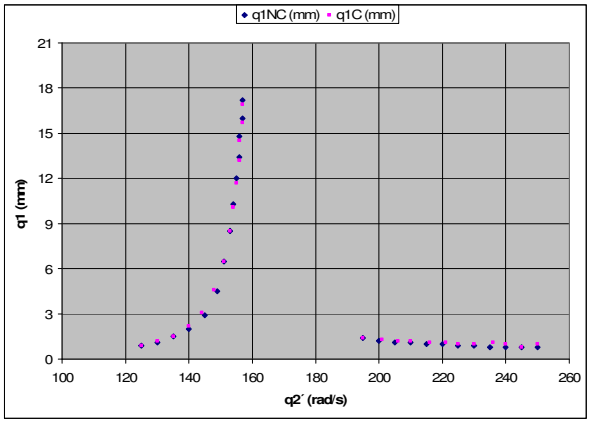

Fig. 10. Resonance curve for non-controlled (NC) and controlled (C) systems for d = 2.0 cm and m_3 = 0.010 kg

We noted that the problem of controlling the vibrations is very sensitive related to the values of d and m_3. If the choice of these values is not adequate, just a few differences will be observed in the resonance curve. It is what we can note in Fig. 10, when we chose values of d = 2.0 cm and m_3 = 0.010 kg. Analyzing the Fig. 10 we note that for a = 0.38 we have the largest value of structure displacement, around 17 mm. So the first tentative of optimizing the carved box, we fixed the value of a equal to 0.38 and solved the optimization problem described by Eqs. (19) to (22), trying to minimize the structure displacement in this region. As the augmented Lagrangian method is iterative, we have to choose an initial design. We started from the initial design {2.0 cm; 0.01 kg; 17 mm}, the values of the design of Fig. 10. The optimum values of the design variables obtained in this case, with 8 iterations, was d = 0.1 cm, m_3 = 0.111 kg. For a = 0.38, the value fixed in this case, we got a really low value of displacement, around 1 mm. It is a significant reduction when we compare with the previous value of 17 mm. But when we plot all the resonance curve, we note that for values of a lower than 0.38 the displacements where very high, reaching max(q_1) = 16 mm when a = 0.37, as we can see in Fig.11. So these results were really good for a = 0.38, but not for other values of a. Regarding this solution, one advantage of it is that we can reach larger values of motor rotation with a smaller power. The jump on the resonance region happens with lower values of energy.

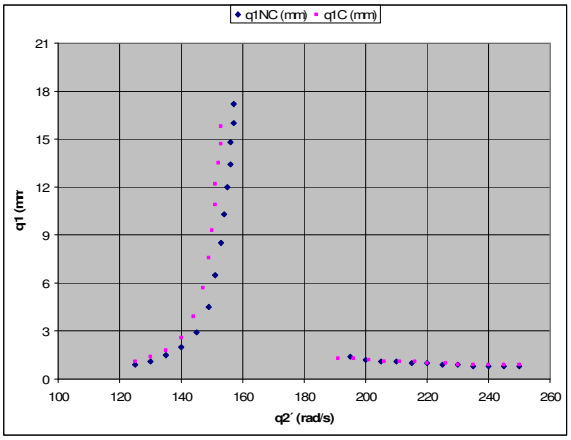

Fig. 11. Resonance curve for non-controlled (NC) and controlled (C) systems for d = 0.1 cm and m_3 = 0.111 kg

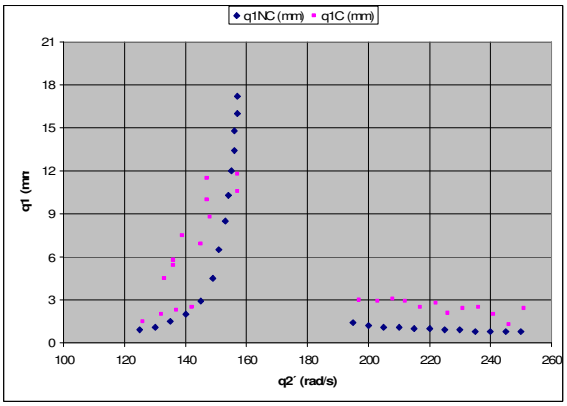

Fig. 12. Resonance curve for non-controlled (NC) and controlled (C) systems for d = 2.8 cm and m_3 = 0.178 kg

In the next tentative of getting an optimum design, starting from the initial design {1.5 cm; 0.183 kg; 14 mm}, we solved the optimization problem described by Eqs. (19) to (22) for all values of a defined previously. We obtained, with 8 iterations, the optimum design with d = 2.8 cm, m_3 = 0.178 kg and max(q_1) = 12 mm, as we can see in Fig.12. We note that the reduction of the maximum displacement before the resonance region is of 31%. This is really significant. But after that, where the motor works with higher frequencies, the increase was of up to 212%, that is, the displacements more than triplicated. Usually, what we expect of a motor is that it will give the maximum power allowable, so this solution may be practical for lower motor frequencies but not for higher frequencies.

Solving the same problem stated above, but starting from the design {3.3 cm; 0.313 kg; 8 mm}, we got, with 8 iterations, the optimum design with d = 0.7 cm, m_3 = 3.881 kg and max(q_1) = 5.8 mm, as we can see in Fig.13.

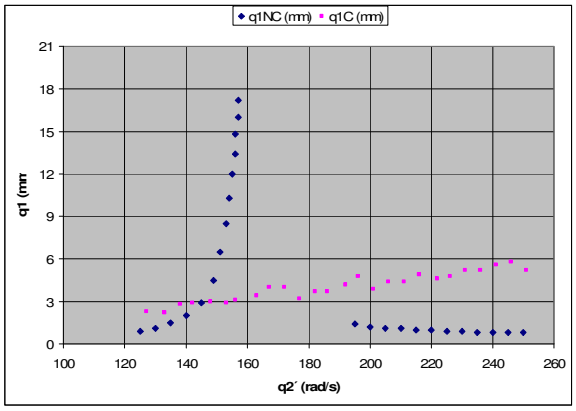

Fig. 13. Resonance curve for non-controlled (NC) and controlled (C) systems for d = 0.7 cm and m_3 = 3.881 kg

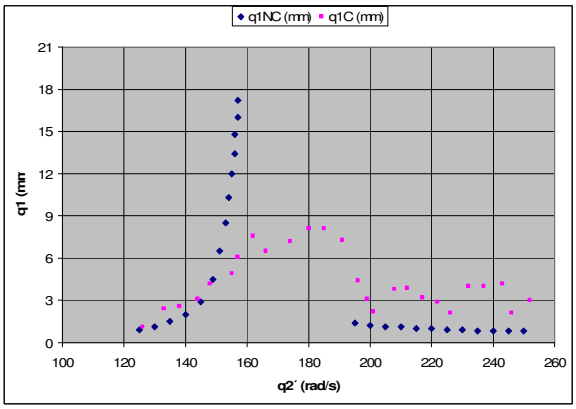

Fig. 14. Resonance curve for non-controlled (NC) and controlled (C) systems for d = 3.3 cm and m_3 = 0.313 kg

What we can see in this design is that it increases drastically the mass of the system, practically triplicates, and reduces the carved gap to millimeters. It means that a relatively big mass was incorporated to the structure. The consequence is that the resonance region disappears, because the equivalent natural frequency of vibration of the system, with all this mass, reduces to around 90 rad/s, that is, out of the plotting region. In practice, this is not viable because a very significant change in the mass of the system is necessary. Regarding the displacements, the design reduces the amplitudes in a part of the curve but increases drastically for higher frequencies, what is not reasonable, as we stated previously. One can note that in all the problems solved until now the augmented Lagrangian method program converged with 8 iterations, which is the minimum number of iterations allowable adopted to the problem.

Now, trying to put more emphasis in the stationary regime, we are going to present the solution of the optimization problem considering the objective function given by Eq. (23) and

constraints functions given by Eqs. (20) to (22). Adopting the initial design {6.0 cm; 0.200 kg; 8 mm}, we got, with 8 iterations, the optimum design with d = 3.3 cm, m_3 = 0.313 kg and max(q_1) = 8.0 mm, as we can see in Fig.14. We can note that this optimum design eliminates the resonance region and reduces the maximum displacement in 53%, but increases the displacements for higher motor frequencies. The values obtained for m_3 and d are very reasonable, since they are easy to be implemented in practice and do not change significantly the mass of the system.

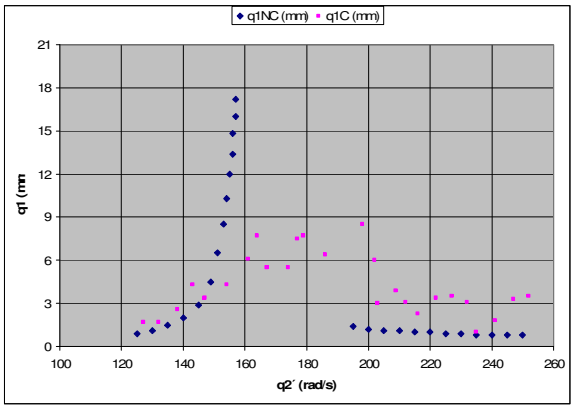

Fig. 15. Resonance curve for non-controlled (NC) and controlled (C) systems for d = 2.7 cm and m_3 = 0.339 kg

Continuing with the strategy of giving more emphasis in the stationary regime, we are going to present the solution of the optimization problem given by the objective function, Eq. (24), and constraint functions given by Eqs. (20) and (21). Note that the number of design variable is now equal to 2 and we have only two constrains applied on the problem. We adopted the initial design {3.3 cm; 0.313 kg}, that is, the optimum design of the problem described previously (Fig. 14). Solving the problem, we got, with 8 iterations, the optimum design with d = 2.7 cm, m_3 = 0.339 kg. For this design the objective function, Eq. (24), is equal to 291. The maximum displacement, in the stationary regime, is 8.5 mm, as we can see in Fig.15. This optimum design also eliminates the resonance region and reduces the maximum displacement in 50%, but increases the displacements for higher motor frequencies. The values obtained for m_3 and d are very reasonable in this case too, easy to be implemented in practice and do not change significantly the mass of the system.

Next, we are going to present the solution of the optimization problem given by the objective function, Eq. (25), and constraint functions given by Eqs. (20) and (21). Note again that in this problem the number of design variable is now equal to 2 and we have only two constrains applied on the problem. We adopted the initial design {2.7 cm; 0.339 kg}, that is, the optimum design of the problem described previously (Fig. 15). Solving the problem, we got, with 8 iterations, the optimum design with d = 7.4 cm, m_3 = 0.102 kg. For this design the objective function, Eq. (25), is equal to 84. The maximum displacement, in the stationary regime, is 8.8 mm, as we can see in Fig.16. This optimum design also eliminates the resonance region, reduces the maximum displacement in 48% and does not increase

significantly the displacements for higher motor frequencies. The values obtained for m_3 and d are very reasonable for practice in this case too.

At this point, we are going to present the solution of the optimization problem given by the objective function, Eq. (26), and constraint functions given by Eqs. (20) and (21). Note that in this problem the number of design variable is now equal to 2 and we have only two constrains applied on the problem. We adopted the initial design {2.7 cm; 0.339 kg}, that is, the design of Fig. 15.

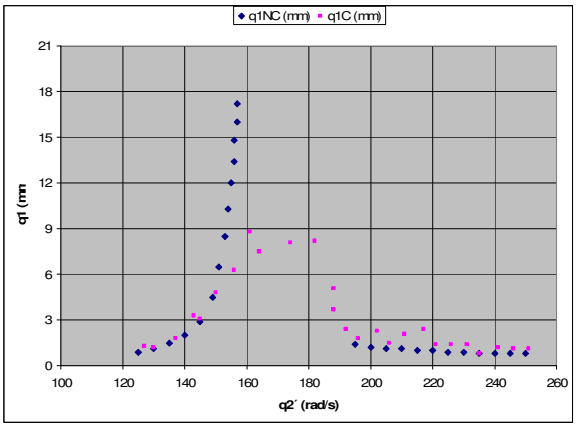

Fig. 16. Resonance curve for non-controlled (NC) and controlled (C) systems for d = 7.4 cm and m_3 = 0.102 kg

Solving the problem, we got, with 8 iterations, the optimum design with d = 10.5 cm, m_3 = 0.049 kg. For this design the objective function, Eq. (26), is equal to 92. The maximum displacement, in the stationary regime, is 10.8 mm, as we can see in Fig.17. This optimum design does not eliminate totally the resonance region, but it reduces the maximum displacement in 36% and does not increase significantly the displacements for higher motor frequencies. The values obtained for m_3 and d are very reasonable for practice in this case too.

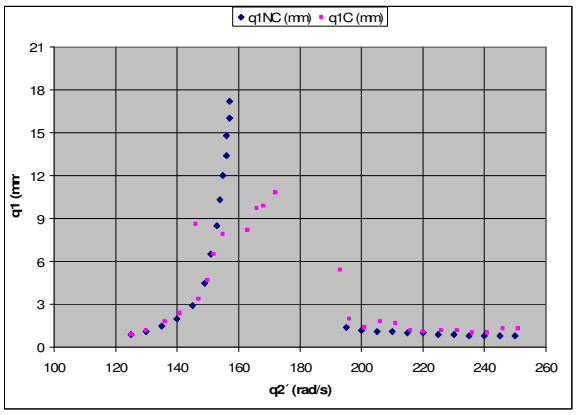

Fig. 17. Resonance curve for non-controlled (NC) and controlled (C) systems for d = 10.5 cm and m_3 = 0.049 kg

We summarized in Table 1 the results obtained in all formulations proposed and solved in the present paper. From the results and comments presented, we can conclude that the formulation considering the objective function given by Eq. (25) was the one that eliminated the resonance region, reduced in 48% the maximum displacement and did not increased substantially the displacements for higher values of motor frequency. In a general way, this formulation presented the best performance. However, if we only consider the displacements for higher motor frequencies the formulation presented by Eq. (26) gave the best result. If we only take in consideration the maximum structure displacement for the reasonable designs obtained, the formulation provided by Eq. (23) gave the best solution.

Status	***a***	**Objective Function**	**Optimum Design**					
			d **(cm)**	m_3 **(kg)**	**Eq. (23)**	**Eq. (24)**	**Eq. (25)**	**Eq. (26)**
NC-RK	0.25-0.50	-	-	-	17.8	791.3	135.8	101.3
NC-NW	0.25-0.50	-	-	-	17.2	682.0	123.4	96.2
C-RK	0.25-0.50	-	2.0	0.010	17.4	767.9	136.5	103.0
C-NW	0.25-0.50	-	2.0	0.010	16.9	662.5	123.8	97.6
C-NW	0.38	Eq. (19)	0.1	0.110	15.8	567.6	114.1	93.8
C-NW	0.25-0.50	Eq. (19)	2.8	0.178	11.8	421.7	121.0	106.0
C-NW	0.25-0.50	Eq. (19)	0.7	3.881	5.8	221.8	104.2	103.3
C-NW	0.25-0.50	Eq. (23)	3.3	0.313	8.1	294.1	112.1	105.0
C-NW	0.25-0.50	Eq. (24)	2.7	0.339	8.5	291.4	110.8	104.1
C-NW	0.25-0.50	Eq. (25)	7.4	0.102	8.8	216.5	84.1	87.4
C-NW	0.25-0.50	Eq. (26)	10.5	0.049	10.8	325.8	97.6	91.7

Table 1 – Summary of the designs obtained in this work

With the intention to have a better visualization of the results obtained, we plotted a 3-D graph (Fig. 18). In this we can see the maximum structure displacement in function of de carved gap (d) and the free mass (m_3). One can note, analyzing those figures, that the mass varying from 0.1 to 0.3 kg and the gap varying from 3 to 7 cm give the minimum values of displacement.

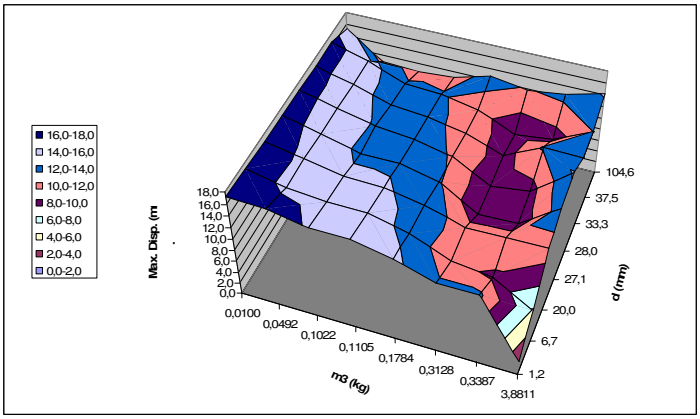

Fig. 18. Maximum structure displacement in function of the carved gap and the free mass values

Other important observation is that when we drastically increase the free mass and reduce the gap the displacements reduce too. As we stated before, it looks like that the free mass was incorporated to the structure.

In a general way, the best values to m_3 varied from 2.5% until 15% of the structure mass and the best value of d varied from 25 until 80 times the static displacement of the structure. However, in problems like the one presented here, where we have a very large range of exciting frequencies (motor frequencies), maybe it should be better to design m_3 and d as a function of the frequency and so develop a system where it can be self adjusted for the optimum values obtained in function of the motor frequency. That is, the gap and the free mass assume a given value which depends on the motor frequency.

7. CONCLUSIONS

The Sommerfeld effect and non-ideal dynamic systems were defined. Several types of impact dampers found in the literature were explained. The equations of motions for the non-ideal system considered here were derived. The augmented Lagrangian method for solving optimization problems with dynamic constrains were presented. Several optimization problems were formulated with the objective to minimize the displacements of the structural system. The design variables of the optimization problems were the free mass and the carved gap of the impact damper, which were properly varied to obtain the optimum design. We solved and commented the results obtained for each optimization problem. We obtained practical designs that reduced the maximum displacements in 50%. We concluded that optimum values of the free mass varied from 2.5% until 15% of the structure mass and the best value of the carved gap varied from 25 until 80 times the static displacement of the structure.

As suggestions for further work we present:

- design an impact damper where the free mass and the carved gap is a function of the frequency and so develop a system where it can be self adjusted for the optimum values obtained in function of the motor frequency;
- optimize an impact damper with the objective of minimizing the displacements of a wind turbine tower.

REFERENCES

[1] Souza, S.L.T., Caldas, I.L., Balthazar, J.M., Brasil, R.M.L.R.F., (2002). Analysis of regular and irregular dynamics of a non-ideal gear-rattling problem. *Journal of the Brazilian Society of Mechanical Sciences* Vol. 24: 111-114.

[2] Souza, S.L.T., Caldas, I.L., Viana, R.L., Balthazar, J.M. and Brasil, R.M.L.R.F., (2005). Impact dampers for controlling chaos in systems with limited power supply. *Journal of Sound and Vibration* Vol. 279: 955-967.

[3] Warminski, J., Balthazar, J.M. and Brasil, R.M.L.R.F., (2001). Vibrations of a non-ideal parametrically and self-excited model. *Journal of Sound and Vibration* Vol. 245: 363-374.
[4] Balthazar, J.M., Brasil, R.M.L.R.F. and Garzeri, F.J., (2004). On non-ideal simple portal frame structural model: experimental results under non-ideal excitation. *Applied Mechanics and Materials* Vols. 1-2: 51-58.
[5] Konenko, V. O., (1969). *Vibrating Systems with Limited Power Supply*. London, Life Books. 236 p.
[6] Popplewell, N., Bapat, C. N. and McLachlan, K., (1983). Stable periodic vibroimpacts of an oscillator. *Journal of Sound and Vibration*, v. 87(1): 41-59.
[7] Bapat, C. N., Popplewell, N. and McLachlan, K., (1983). Stable periodic motions of an impact-pair. *Journal of Sound and Vibration*, v. 87(1): 19-40.
[8] Duncan, M. R., Wassgren, C. R. and Krousgrill, C. M., (2005). The damping performance of a single particle impact damper. *Journal of Sound and Vibration*, v. 286: 123-144.
[9] Bapat, C. N. and Sankar, S., (1985). Single unit impact damper in free and forced vibration. *Journal of Sound and Vibration*, v. 99(1): 85-94.
[10] Popplewell, N. and Liao, M., (1991). A simple design procedure for optimum impact dampers. *Journal of Sound and Vibration*, v. 146(3): 519-526.
[11] Saeki, M., (2002). Impact damping with granular materials in a horizontally vibrating system. *Journal of Sound and Vibration*, v. 251(1): 153-161.
[12] Marhadi, K. S. and Kinra, V. K., (2005). Particle impact damping: effect of mass ratio, material and shape. *Journal of Sound and Vibration*, v. 283: 433-448.
[13] Popplewell, N. and Semercigil, S. E., (1989). Performance of a beam bag impact damper for a sinusoidal external force. *Journal of Sound and Vibration*, v. 133(2): 193-223.
[14] Feitosa, L. C. S., (2006), *Controle por Impacto de Vibrações Estruturais Excitadas por Carregamentos Não-Ideais*, "In Portuguese". Master Dissertation, Polytechnic School of The University of Sao Paulo, Sao Paulo, Brazil, 120 p.
[15] Arora, J. S., Chahande, A. I., and Paeng, J. K., (1991). Multiplier methods for engineering optimization. *Int. J. Numer. Methods Eng.,* 32, 1485–1525.
[16] Chahande, A. I., and Arora, J. S., (1994). Optimization of large structures subjected to dynamic loads with the multiplier method. *Int. J. Numer. Methods Eng.,* 37, 413–430.

ACKNOWLEDGMENTS

This work is result of research projects of Post-Doctorate accomplished by Marcelo Araujo da Silva, under the supervision of Prof. Dr. Reyolando M. L. R. F. Brasil. The work was carried out at The University of Sao Paulo, in Sao Paulo-SP., Brazil, and at The University of Iowa, in Iowa City-IA, USA. The programs were sponsored by FAPESP under the Projects N.º 2005/02815-5 and 2006/04744-0. All these supports are gratefully acknowledged.